Desalination and Water Treatment
www.deswater.com
doi: 10.1080/19443994.2015.1101718

57 (2016) 19713–19726
September

Taylor & Francis
Taylor & Francis Group

Treatment of surfactant-stabilized oily wastewater using coalescing bed of bagasse fly ash (BFA) as a low-cost filter medium: modelling and optimization of process parameters

Partha Kundu[a], Indra Mani Mishra[a,b,*]

[a]*Department of Chemical Engineering, Indian Institute of Technology Roorkee, Roorkee, Uttarakhand 24766, India, Tel. +91 1332 286637; email: partha_dch12@outlook.com (P. Kundu), Tel. +91 326 2235227; Fax: +91 326 2296563; email: immishra49@gmail.com (I.M. Mishra)*
[b]*Department of Chemical Engineering, Indian School of Mines, Dhanbad, Jharkhand 826004, India*

Received 18 April 2015; Accepted 25 September 2015

ABSTRACT

In the present study, surfactant-stabilized oily wastewater was separated using a low-cost agricultural waste, bagasse fly ash (BFA) in a packed coalescing bed. Factors such as pH (*A*), BFA bed height (*B*) and flow rate of emulsion (*C*) were the most significant process parameters, affecting the oil separation efficiency by the BFA coalescing bed. The effect of the above parameters on the removal efficiency of BFA coalescing bed was investigated by three-level-three-factor (3^3) Box–Behnken Design model using response surface methodology. A second-order polynomial model equation was proposed with a high correlation coefficient ($R^2 = 0.9942$), which explained the parametric interactions significantly well. About 84.8% of oil removal efficiency was achieved under optimal parametric conditions: pH_0 3, 100 mm bed height and 0.145 dm^3/min flow rate. BFA, being almost a free waste material, can be effectively used for the treatment of oily wastewaters.

Keywords: Wastewater treatment; Oily wastewater; Bagasse fly ash (BFA); Low-cost filter media; Oil removal; Optimization

1. Introduction

Large volumes of oily wastewaters are discharged from various operations and processes connected with crude oil/gas production from reservoirs, petroleum refining, petrochemical units, flue gas scrubbing unit, oil dispensing unit, etc. [1]. Oil field wastewaters are also produced in large quantities from the site of onshore and offshore oil exploitation. These oily wastewaters contain a number of hydrocarbons, surfactants and oils in the form of emulsions. The treatment and disposal costs are increasing day by day due to the production of large volume of oily wastewaters. Resource recovery is a very important part of the waste management programme. With an increasing price of crude oil, the goal must be the recovery of every usable barrel of oil. Therefore, an efficient and cost-effective treatment process must be implemented for the separation of emulsified oil from wastewaters.

Oil and water are immiscible in each other. As the oil is mixed with water, it forms either an immiscible floating layer of oil or an oil-in-water/water-in-oil (o/w or w/o) emulsion in the presence of a surfactant(s) [2].

*Corresponding author.

The o/w or w/o emulsion is stabilized, due to the existence of thin interfacial films of the surfactant and the mutual electrostatic repulsion among the similarly charged dispersed droplets [3,4]. The discharge of this oily wastewater into the water body without any treatment causes serious environmental problems. The oily layer or emulsion impedes the natural oxygenation process of aquatic environment as also the solar irradiation penetrating the water body. Since the oily wastewater is not readily biodegradable, even a low concentration of oil in emulsion form is toxic to the flora, fauna and micro-organisms. Therefore, it is detrimental to the aquatic ecology. The oil concentration in the wastewater from an oil field generally varies from 100 to 1,000 mg/l [5]. The environmental regulating agencies of various countries have set a discharge limit of oil concentration in the wastewater into the surface water. The Ministry of Environment, Forest and Climate Change (MoEFCC), Government of India, has set a limit of 5 mg/l of oil concentration in the discharge waters for sewers and surface waters [6].

There are a number of physical–chemical methods for the removal of emulsified oil from oily wastewaters [7–10]. Among these methods, deep-bed filtration and packed-bed oil coalescence are reported to be very efficient [7–12]. The feasibility of fixed beds, to a large extent, depends on the cost of the filter media and their availability. Several filter media have been used in lab-scale studies which include peat [11,12], inorganic oxides [13], saw dust [14] and sand [15]. Membrane filtration (MF), microfiltration and ultrafiltration (UF) are also suggested for the treatment of oily wastewaters [16]. Mueller et al. [17] used alumina ceramic membranes and a surface-modified polyacrylonitrile membrane for the treatment of oily water. Abbasi et al. [18] used mullite ceramic microfiltration Membranes for oily wastewater treatment. However, the membrane fouling caused by the accumulation of oil and surfactant molecules reduces the permeate flux of the membrane, thereby limiting the applicability of the process. The cost of the membrane is also an important factor.

Adsorption is a reversible separation technique which is used for the treatment of emulsified wastewater. In such a process, the adsorbed molecules attach to the surface by hydrogen bonding having much lower bond energy than the surface ionic bond energy [19]. These make the process reversible for the separation and recovery of adsorbed molecules simultaneously by breaking the hydrogen bonding between the surface and the adhering molecule. A packed bed with an oil coalescing media is used for the effective treatment of oily wastewater (o/w emulsions) with an appropriate oil droplet size [9,10,20,21]. However, the oil coalescing media are quite costly and their cyclic regeneration reduces their effectiveness. The search for a cost-effective filter media leads to the use of agricultural wastes, such as bagasse fly ash (BFA), rice husk ash (RHA) and saw dust (SD) for the treatment of oily wastewaters because of their high oil removal efficiency and their relatively low costs. BFA is available in abundance, at almost no cost, from the sugar cane-based sugar mills, wherein bagasse is used as the fuel for boiler furnaces. It has very high sorption capacity for heavy metals and volatile organics like phenol, pyridine, acrylic acid, acrylonitrile and their derivatives[22–27].

Oily wastewaters are generally treated and filtered through fixed-bed columns. System pH, particle size and shape, bed height and oil concentration in the emulsion play very important roles in the oil-droplet coalescence and subsequent oil removal. It is, therefore, necessary to optimize the system parameters for the optimal removal of oil. The basic objective is to evaluate those parameters that have appreciable impact on the process of oil separation and its eventual removal. The multi-parameter optimization methods are time-consuming, and they also ignore the inter-parametric interaction effects. Hence, the system does not reach the actual optimum condition for the process under investigation. It is, therefore, imperative to use the statistical design of experiments with a minimum number of experiments so as to obtain the desired information [16]. Box–Behnken design (BBD) model using response surface methodology (RSM) is effective in designing experiments, modelling and discerning statistically all the possible impacts of individual parameters and inter-parametric interactions [10,27–29]. In the present work, the feasibility of using the BFA coalescing bed as a low-cost filter medium, for the treatment of oily wastewater is investigated. The experimental design and modelling were carried out using BBD under RSM. The effect of significant process parameters, such as the system pH (*A*), bed height (*B*) and flow velocity (*C*) on the oil removal efficiency of BFA filter bed has been investigated. The cost of various filter media is also discussed.

2. Materials and methods

2.1. Adsorbent and adsorbate

BFA was obtained from Uttam Sugar Mills, UP (India). At first BFA was thoroughly cleaned by washing it with hot Millipore water (70–80 ℃) and then dried in a hot air oven. Thereafter, the BFA particles were sieved using IS sieves [30,31]. The proximate analysis and chemical analysis of the sieved BFA were carried out using standard methods prescribed by the Bureau of Indian Standards [30,31]. The bulk density of BFA was determined by a bulk density meter. CHN

analysis was done using Perkin-Elmer CHN elemental analyzer. The detailed surface area analysis and pore size distribution of BFA were carried out by N_2 adsorption isotherm technique using ASAP 2020 Micromeritics instrument and Brunauer–Emmett–Teller (BET) method. The physical–chemical characteristics of the BFA are shown in Table 1.

A scanning electron microscope (Model Leo, 4 3SVP) was used to obtain the micrographs of BFA particles. FTIR spectrometer (Nicolet Model Avtar 370 Csl, Thermo Electron Corporation, USA) was used for obtaining Fourier transformed infrared (FTIR) spectra of virgin and oil-loaded BFA.

The oily wastewater in the form of o/w emulsions was prepared synthetically The o/w emulsion was prepared by mixing hydrocarbon fuel oil, procured from an oil-dispensing unit, reverse osmosis water and an anionic surfactant, sodium dodecyl benzene sulphonate (SDBS), and stirred at 5,000 rpm using a laboratory stirrer (Remi) for 10 min. The o/w emulsion was prepared with a constant oil concentration (30% v/v) and surfactant concentration (0.5% w/v) in water. The stability of the emulsion was determined by observing the relative volumes of the phases which got separated after 24 h storage in a temperature-controlled vessel.

2.2. Thermal stability analysis (TGA/DTG/DTA) of BFA

Thermal analysis of both the virgin and loaded BFA was carried out by thermogravimetry using a

Table 1
Physical–chemical characteristics of BFA

Characteristics	Value	
Proximate analysis (%)	Fresh BFA	Spent BFA
Moisture	3.41	9.63
Volatile matter[a]	23.73	24.86
Ash[a]	28.47	28.82
Fixed carbon[a]	44.39	36.69
Bulk density (kg/m^3)	242	–
Lower heating value (MJ/kg)	22.531	24.862
Particle size (μm)	200–275	
Ultimate analysis (dry basis) (%)		
C	16.87	
H	10.11	
N	2.31	
S	–	
Chemical analysis of ash (%)		
SiO_2	54.21	
Al_2O_3	10.58	
Fe_2O_3	2.63	
CaO	6.78	
MgO	1.82	
Surface area of pores (m^2/g)		
(1) BET surface area	171.42	
(2) BET adsorption cross-sectional area (nm^2)	0.162	
(3) *t*-plot micropore area	46.321	
BJH cumulative pore volume (cm^3/g)		
BJH adsorption	0.03776	
BJH desorption	0.03654	
Average Pore size (Å)		
BET	27.53	
BJH adsorption	38.42	
BJH desorption	37.12	
Porosity	0.65	

[a]Moisture-free basis.

Perkin-Elmer-Pyris Diamond TG instrument at a heating rate of 283 K/min from ambient temperature to 1,273 K using alumina powder (10.5 mg) as the reference material. The thermal degradation runs were taken in an oxidizing environment at an airflow rate of 300 ml/min.

2.3. Point of zero charge (pH_{PZC}) of BFA

The surface charge of BFA was determined by the solid addition method given elsewhere [10].

2.4. Chemicals

The chemicals used in the present study were procured from different companies as shown within brackets: sodium hydroxide (RFCL, New Delhi), sulphuric acid (Rankem, New Delhi), hydrochloric acid (Rankem, New Delhi), n-hexane (RFCL, New Delhi), anhydrate sodium sulphate (Rankem, New Delhi), SDBS (Himedia, Mumbai), sodium chloride (SRL, Mumbai), sodium carbonate (NICE, Cochin) and hydrocarbon fuel oil (Indian Oil Corporation Ltd). All the chemicals, except hydrocarbon fuel oil, were of analytical reagent grade.

2.5. Estimation of oil concentration

The oil concentration in the emulsions and other liquid mixtures was estimated by spectrophotometry method using FTIR spectrophotometer. For each estimation, the emulsified wastewater sample was adjusted to pH 2. The sample was then placed in an Erlenmeyer flask with CCl_4 as the solvent, and shaken for 10 min in a laboratory shaker. Thereafter, the mixture was put in a separating funnel for the separation of the oily phase and the aqueous phase. A filter paper (blue ribbon) containing 1 g of anhydrous Na_2SO_4 was used for the filtration of the solvent–oil phase and the aqueous phase. The IR spectral range of 2,700–3,200 cm^{-1} was used for scanning. Typical absorption peaks were observed for various hydrocarbon groups. The heights of all absorption peaks ($-CH_3$, 2,959 cm^{-1}; $-CH_2$, 2,954 cm^{-1}; $-CH$, 3,030 cm^{-1}) were summed up for estimating the total oil concentration. Oil concentration was determined as [10]:

$$C_{oil} = \frac{CV_{Sol}}{V_{Sample}} \quad (1)$$

where C_{oil} is the oil concentration (mg/dm^3), C is the unknown oil concentration obtained from the calibration curve (mg/dm^3), V_{sol} the volume of the solvent (CCl_4) used for extraction (dm^3) and V_{sample} is the volume of the emulsified wastewater sample (dm^3).

The oil removal efficiency of the BFA filter bed was estimated from the following equation:

$$\eta = \frac{C_i - C_0}{C_I} \times 100 \quad (2)$$

where η = oil removal efficiency (%), C_i = feed oil concentration (mg/dm^3), and C_0 = bed outlet oil concentration (mg/dm^3).

2.6. Measurement of droplet size and zeta potential of o/w emulsions

Emulsion droplet size of the freshly prepared emulsion was measured by Zetasizer (Malvern Nano ZS 90, UK) using dynamic light scattering (DLS) technique at room temperature (25˚C). The freshly prepared emulsion was diluted by Millipore water and transferred into the transparent polystyrene cuvette up to the mark. The filled cuvette was placed inside the Zetasizer and the droplet size distribution was obtained in terms of percent number density. The zeta potential of the o/w emulsions was also obtained by the same instrument using a disposable folded polystyrene capillary cell.

3. Experimental procedure

A synchronized approach has been adopted in the present work. The significant parameters affecting the system were identified and the experiments were performed according to BBD matrix to find out the actual response (oil removal efficiency). Based on statistical analysis (analysis of variance (ANOVA)), a model was developed and the model predictions were then compared with the actual experimental response. The design of experiments was synthesized with the experimental methods, parameters and the results are discussed accordingly.

3.1. Experimental set-up

The filtration unit consists of three distinct sections; inlet section at the bottom (135 mm), coalescing section in the middle (120 mm) and decantation section at the top of the unit (145 mm). The filtration unit was fabricated by plexiglass pipes having a wall thickness of 10 mm, an inside diameter of 140 mm and the total height of 400 mm. The inlet section is packed with glass beads of 10 mm size for facilitating

the cross-sectional velocity of the feed stream to have flat velocity profile while entering the coalescing section and to avoid any entrance effect. The decantation section was free of any packing. The coalescing section was packed with BFA particles. The separated oil and the supernatant water were collected from the respective outlets separated by an interval of 50 mm. The design was modular, and a number of modules of packing could be joined one above the other. All the sections were joined with the help of flanges made from the acrylic sheets (Fig. 1). The accessories associated with the filtration unit are shown in Fig. 1. The emulsion feed tank is equipped with an agitator for continuous mixing to maintain the homogeneity of the emulsified feed water. The emulsified wastewater was pumped from the emulsion feed tank to the filtration unit using a peristaltic pump.

3.2. Experimental and statistical design

A three-level, three-factorial (3^3) BBD was used to optimize the number of experiments for investigating the effects of process parameters on the oil removal efficiency of the BFA filter bed. The ranges of input variables were chosen as: pH (2–10), bed height (400–120 mm) and flow velocity (0.135–0.270 dm^3/min). The oil concentration of 30% (v/v) was used as the constant input parameter. The input variables were codified as: −1 (low), 0 (central point or middle) and 1 (high). The experimental design and the statistical analysis were performed using the Design-Expert software® (V.8, Stat Ease Inc., Minneapolis, USA). Higher order polynomial equations were rigorously fitted to the experimental data to obtain the desired model equations for the BFA filter bed. The functional relationship between the response (Y) and the input process variables is represented as follows:

$$Y = g(x_1, x_2, x_3, ...x_m) + \varphi \quad (3)$$

where $g(x_i)$ is the real response function and ϕ is the residual error. The quadratic response model for predicting the optimal conditions and for identifying the relevant terms is given as follows:

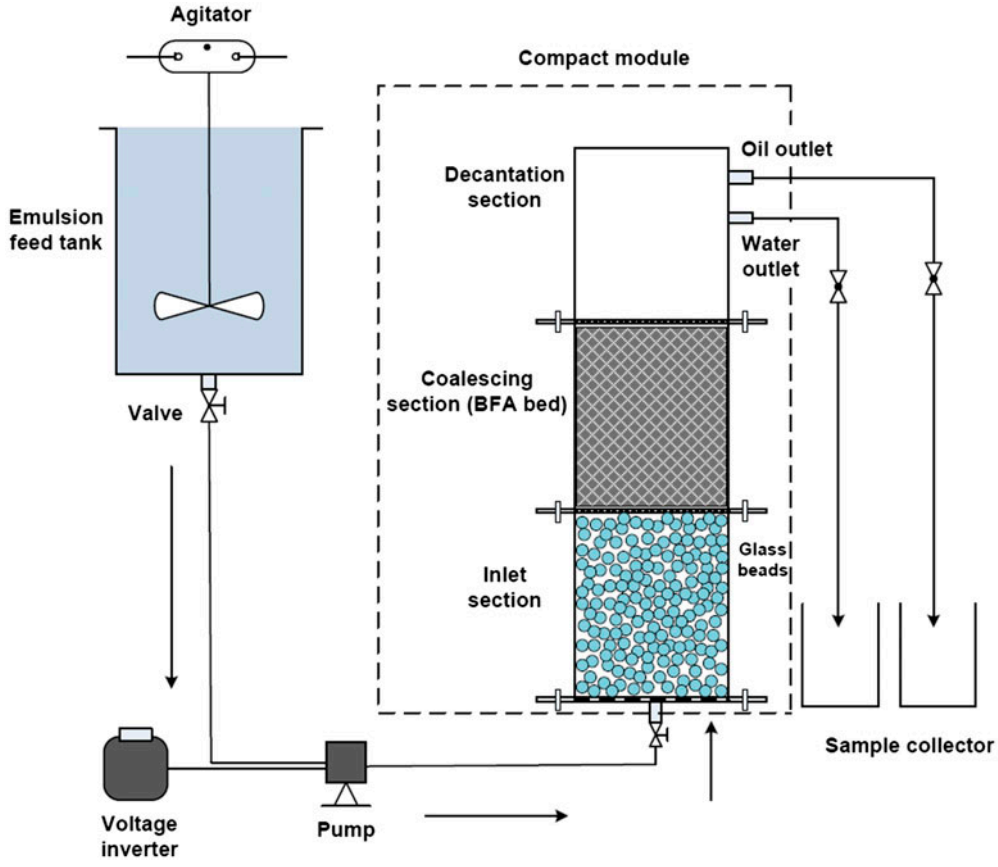

Fig. 1. Schematic diagram of BFA bed coalescing system.

$$Y = \alpha_0 + \sum_{i=1}^{m} \alpha_i \,.\, x_i + \sum_{i=1}^{m} \alpha_{ii} \,.\, x_{ii}^2 + \sum_{i_i \le j}^{m} \sum_{j}^{m} \alpha_{ij} \,.\, x_i . x_j + \cdots + \varphi_r \tag{4}$$

where i is the linear coefficient, j is the quadratic coefficient, α_0 is the intercept, α_i is the linear coefficient of the input factor x_i, α_{ii} is the squared coefficient between the input factor x_i and x_j, α_{ij} is the quadratic coefficient of input factor x_i, m is the number of experimental factors studied and optimized and φ_r is the random error [26–29].

4. Result and discussion

4.1. BFA filter media characterization

The physical–chemical properties of BFA particles are shown in Table 1. It can be seen that the BFA has a large surface area and porosity. The pore size (pore volume and area) distribution of BFA particles are shown in Fig. 2. The pore size distribution shows that the majority of pores fall in the mesoporous range (20–50 Å). The micropores (<20 Å) account for 26.4% of the total pore surface area, while the mesopores account for 73.6% of the area. The wide pore size distribution exhibits the surface heterogeneity of the BFA particles. The BET average pore size is 27.53 Å with a BET pore surface area of 171.4 m^2/g.

The SEM micrographs (Fig. 3) show the morphological changes that occurred from the virgin BFA particles to emulsion-loaded particles. It is observed from Fig. 3 that the surface texture and the pore size of the loaded BFA particles change drastically from that for virgin particles. BFA was characterized by large-sized fibrous particles. The SEM micrograph of virgin BFA shows transparent surface texture, which indicates the active sites present on the virgin BFA surface. Fig. 3(a) shows the presence of a large number of active sites in the virgin BFA particles. Fig. 3(b) shows that most of the active sites of BFA particles are totally filled by emulsified oil. As the o/w emulsion passes through the BFA bed, dispersed oil droplets adhere to the active sites of the BFA particles. The oil droplets are adsorbed over the free surface of BFA particles and form a thinly adsorbed oily layer over the BFA surface. The oily layer gradually thickens with time, as more and more emulsified oil droplets interact with the BFA bed.

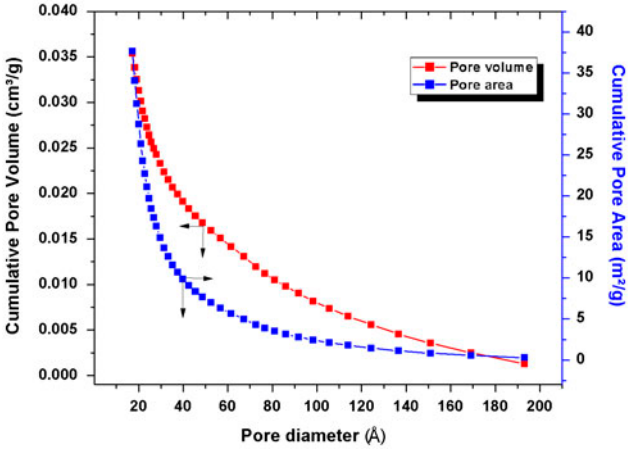

Fig. 2. Pore size distribution of virgin BFA.

The functional groups of the adsorbed hydrocarbons (from oil) on BFA particles were identified by the FTIR spectra. Fig. 4(a) and (b) shows the FTIR spectra of virgin and the loaded BFA particles. A broad band for both virgin and loaded BFA particles between 3,253 and 3,563 cm^{-1} indicates the existence of free and hydrogen-bonded –OH groups on the BFA surface. The bond stretching is mainly because of the silanol groups (Si–OH) and adsorbed water molecules (3,400 cm^{-1}) on the BFA surface [31]. Absorption peaks (Fig. 4(a)) at 1,344 and 1,379 cm^{-1} for virgin BFA particles are due to −CH bending vibration. Peaks at 1,584, 1,605 and 1,634 cm^{-1} are due to the conjugated C=C groups and C=O groups, respectively.

During the passage of o/w emulsion stream through the BFA filter bed, emulsified oil droplets get adsorbed, fill the pores and form an oily layer around the external surface of the particles. The occurrence of adsorption was manifested in Fig. 4(b). Peaks at 1,348 and 1,364 cm^{-1} are ascribed to –CH bending vibration, 1,381 cm^{-1} for $–CH_3$ groups, 1,446–1,450 cm^{-1} for non-conjugated C=C groups, 1,593 cm^{-1} for conjugated C=C groups and 1,606 cm^{-1} for aromatic groups. Significant adsorption of oil molecules on the BFA surface was observed by the appearance of a large number of IR spectral peaks within the range of aliphatic and aromatic hydrocarbons. Absorption peaks at 2,852, 2,934, 2,958 and 2,862 cm^{-1} are due to the –CH stretching vibration of aliphatic hydrocarbons and 2,925 cm^{-1} due to the methylene groups ($–CH_2$), respectively.

4.2. Thermal analysis of virgin and loaded BFA

Thermal stability of BFA particles was analysed by observing the variation of the decomposition temperature of its associated oxides and functional groups. In thermal stability analysis, samples were heated to moderate to high temperature. During heating, the surface compounds decompose and produce CO

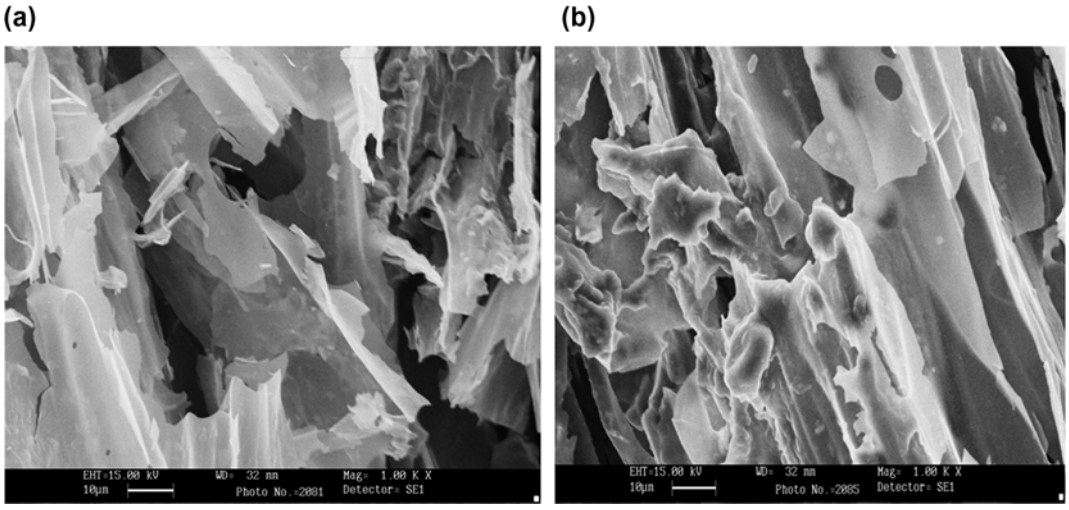

Fig. 3. SEM of (a) virgin BFA and (b) oil-loaded BFA at 1.00 Kx.

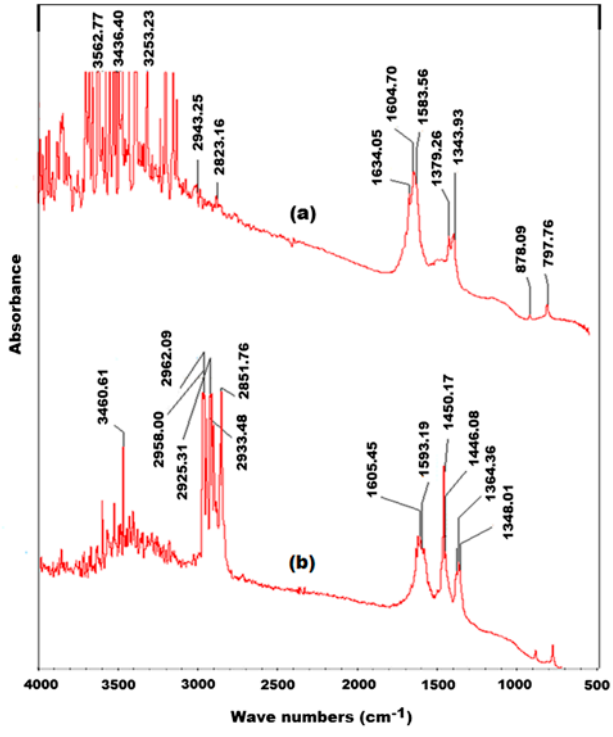

Fig. 4. FTIR spectra of (a) virgin BFA and (b) oil-loaded BFA.

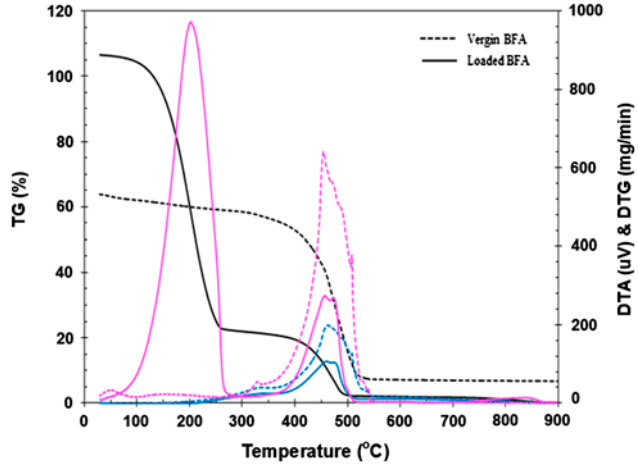

Fig. 5. TG, DTA, DTG plots of unloaded and loaded BFA. TG (–), DTA (–) and DTG (–).

(200–600˚C), CO_2 (450–1,000˚C), water vapour and free hydrogen (500–1,000˚C) [32]. The results of the thermogravimetric analysis of virgin and loaded BFA particles under oxidizing environment at a heating rate of 10 K/min are shown in Fig. 5. Three different thermal decomposition zones are seen in the TG/DTG/DTA traces. From TG thermograph, it is observed that the virgin BFA loses about 70% of its mass in the second temperature zone (400–523˚C). In the first (25–400˚C) and third zones (523–1,000˚C), the mass losses are relatively smaller, i.e. 17.2 and 2.5%, respectively. For the loaded BFA particles, a maximum weight loss of ~64% occurred in the first zone (25–264˚C) which corresponds to the removal of adsorbed oil, moisture and light volatile species from the BFA. Thereafter, ~29% weight loss took place in the second zone (265–480˚C), due to the active pyrolysis and oxidation of the remaining bound oil molecules within the pores. In the third zone (481–1,000˚C), samples show gradual but steady weight loss up to 700˚C, due to evolution of CO_2 and CO. About 1% residue was obtained at 1,000˚C. It can be inferred that

the silicon and aluminium oxides formed, which are relatively stable even at higher temperatures [33].

In DTA trace, the exothermic peak appears at ~450˚C, which indicates the oxidative degradation of the virgin BFA. For loaded BFA, a broad exothermic peak is seen in the temperature range of 400–500˚C. A broad peak appearing in the DTA trace indicates the combustion of carbon species, as shown in Fig. 5. The DTG spectra of loaded BFA particles show a peak at 200˚C, which indicates the vaporization loss of adsorbed oil.

4.3. Surface charge of BFA

The surface charge (point of zero charge, PZC) of BFA is found to be ~7.8, as shown in Fig. 6. At pH < PZC, the BFA surface is positively charged, due to the donor/acceptor interactions between the hydronium ions, and the carbon graphene layers on BFA surface [23,34]. Each adsorbent–adsorbate system is unique about its mutual affinity/reactivity and must be considered in each case separately. The adsorption of positively charged ions are favoured at pH > PZC, and that of the negatively charged ions at pH < PZC. When the pH of emulsion is less than PZC, most of the BFA surface becomes positively charged and the negatively charged oil droplets are attached to the BFA surface. Hence, the system pH < PZC favours oil splitting from the emulsion and the oil adsorption and filtration by the BFA bed.

4.4. Droplet size distribution of o/w emulsions

The average emulsion droplet size of o/w emulsions is found to be 1.2 μm. The droplet size distribution of the o/w emulsion covers the size range from 0.1 to 40 μm. A bimodal type of droplet size distribution is observed.

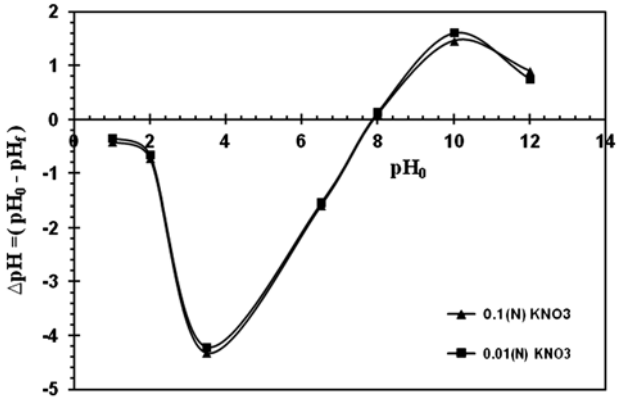

Fig. 6. Point of zero charge, $pH_{PZC,}$ of BFA filter bed.

4.5. Process modelling and Statistical analysis

The individual and combined effects of significant process parameters, i.e. pH, bed height and the emulsion flow velocity on the oil removal efficiency of BFA filter bed are investigated using the BBD model. The RSM is used to measure the response (Y) according to the design matrix as shown in Table 2.

The significance level of process parameters are analysed by employing the ANOVA as shown in Table 3. The Fisher's $F_{Statistics}$ values were found to be large for all the regressions. This indicates the applicability of the regression equation in explaining most of the variations in the response. The model F-value is 287.7, which implies that the model is highly significant. The probability "Prob. > F" less than 0.05 indicates that the model terms are significant. The significant parameters were found to be A, B, C and A^2, B^2, C^2. The predicted and the adjusted values of R^2 are 0.9771 and 0.9908, respectively. These values are very near to one, and are comparable. Thus, a high correlation exists between the experimental and the model predicted values which indicate the fitness of the model.

The selection of an adequate model for the BFA filter system was shown in Table 3. The $p > F$-value for the quadratic model is found to be <0.05 as compared to the 2FI and the linear models. The model summary statistics show that the quadratic model has very high R^2, Adj. R^2 and Pre. R^2 values as compared to the respective values for the linear and 2FI models. Hence, the quadratic model is chosen for the BFA filter bed system.

The ANOVA for the BFA filter bed showed a linear and quadratic relationship between the significant process parameters such as pH, bed height and flow rate. The design model equation for the maximum oil removal efficiency (C.I > 95%) is found to be:

$$Y = 76.78 - 8.49A + 5.20B - 3.51C - 2.18A^2 - 4.70B^2 - 1.13C^2 \quad (5)$$

Fig. 7(b) shows a normal probability vs. residual error plot. The data points lie close to the straight line, which signifies that A, B, C, and A^2, B^2, C^2 are the significant parametric interactions which satisfy the assumptions of the analysis. Fig. 7(b) shows that the developed model is adequate, since the residuals appear to be close to the diagonal line with minimum residuals. Actual and the predicted values of the response are shown in Fig. 7(c).

Table 2
Experimental values of three-level BBD with three independent variables

Std. run order	*A*: pH	*B*: Bed height (mm)	*C*: Flow rate ($dm^3/min \times 10^3$)	Oil removal efficiency, *Y* (%)		Percentage error, ε (%)
				$Y_{experimental}$	$Y_{predicted}$	
1	10 (1)	80 (0)	135 (–1)	68.7	68.5	0.292
2	6 (0)	80 (0)	202.5 (0)	76.8	76.7	0.130
3	2 (–1)	120 (1)	202.5 (0)	83.5	83.59	−0.108
4	6 (0)	40 (–1)	135 (–1)	69.5	69.26	0.347
5	10 (1)	40 (–1)	202.5 (0)	57.2	56.21	1.761
6	2 (–1)	80 (0)	270 (1)	79.5	78.45	1.338
7	10 (1)	80 (0)	270 (1)	60.1	61.48	−2.245
8	6 (0)	120 (1)	270 (1)	73.1	72.64	0.633
9	6 (0)	80 (0)	202.5 (0)	76.6	76.76	−0.208
10	6 (0)	80 (0)	202.5 (0)	76.8	76.76	0.052
11	2 (–1)	40 (–1)	202.5 (0)	72.1	73.19	−1.490
12	6 (0)	120 (1)	135 (–1)	79.1	79.66	−0.703
13	6 (0)	80 (0)	202.5 (0)	76.8	76.76	0.052
14	6 (0)	40 (–1)	270 (1)	62.1	62.24	−0.225
15	6 (0)	80 (0)	202.5 (0)	76.9	76.76	0.182
16	10 (1)	120 (1)	202.5 (0)	66.8	66.61	0.285
17	2 (–1)	80 (0)	135 (–1)	85.6	85.48	0.141

4.6. Optimization of process parameters

The goal of the present study was to maximize the oil removal efficiency. The numerical optimization was done using the desirability approach by introducing a desirability function or objective function, $D(X)$. The simultaneous objective function or total desirability is defined as a geometric mean of all transformed responses [35]:

$$D(X) = (d_1(Y_1) \times d_2(Y_2) \times \cdots \times d_n(Y_n))^{\frac{1}{n}} = \left(\prod_{i-1}^{n} d_i(Y_i)\right)^{\frac{1}{n}} \quad (6)$$

where n is the number of responses in the measure and d_i is the ith desirability. $D(X)$ lies between 0 and 1. It should be noted that, if any of the responses or factors fall outside their desirability range ($d_i(Y_i) = 0$), the overall function becomes zero. The optimization criteria used for obtaining the final optimum solution is illustrated as follows:

$$Y(x_i)|_{\rightarrow \text{maximize}} = \left.\begin{array}{c} -1 \leq A \geq +1 \\ -1 \leq B \geq +1 \\ -1 \leq C \geq +1 \end{array}\right\} \quad (7)$$

The parametric constraints and the optimum results with total desirability of 0.989 are shown in Table 4. Additional experiments in triplicate were carried out at the optimum conditions, in order to check the accuracy and the validity of the predicted optimum conditions. The oil removal efficiency (response) of the BFA bed was found to be consistent with the optimum value, showing a deviation of ~2.22%. This reflected that there was good agreement between the experimental and the predicted values. The experimental results confirmed the validity of the proposed BBD model for maximizing the oil removal efficiency of the BFA filter media.

4.7. Mechanism of oil separation by BFA filter bed

The coalescence phenomena of oil droplets in the BFA filter bed involve three major steps: Brownian diffusion, interception and impaction. The interception mechanism is the most important mechanism in the coalescence process. Once an oil droplet reaches a BFA particle, it gets attached to and spreads over the BFA surface. The BFA particles act as a fibrous coalescer while capturing the suspended oil droplets that grow on the fibrous matrix by further capture and coalescence until they eventually become so large that hydrodynamic drag causes the deformation of the droplets, leading eventually to the breakaway/disintegration of the droplets. The size of the emulsion droplets varies in the range of 0.1–40 μm with an average droplet size of 1.2 μm, which can be effectively captured by the BFA particle surface. The interfacial tension is

Table 3
ANOVA and model statistics of response surface quadratic model (*Y*) for BFA filter bed system

Source	Sum of squares	df	Mean square	*F*-value	$p > F$	Remarks
Model	1,018.91	6	169.82	287.68	<0.0001	Highly significant
A-pH	576.30	1	576.30	976.29	<0.0001	Significant
B-Bed height	216.32	1	216.32	366.46	<0.0001	Significant
C-Flow rate	98.70	1	98.70	167.21	<0.0001	Significant
A^2	19.96	1	19.96	33.82	0.0002	Significant
B^2	93.11	1	93.11	157.73	<0.0001	Significant
C^2	5.35	1	5.35	9.07	0.0131	Significant
Residual	5.90	10	0.59	–	–	–
Pure error	0.048	4	0.012	–	–	–
Cor total	1,024.82	16	–	–	–	–
$R^2 = 0.9942$; Adjusted $R^2 = 0.9908$; Predicted $R^2 = 0.9771$; Adequate precision = 59.354						
Sequential model sum of squares						
Mean vs. Total	90,622.20	1	90,622.20	–	–	–
Linear vs. Mean	891.32	3	297.11	28.93	<0.0001	Suggested
2FI vs. Linear	2.86	3	0.95	0.073	0.9731	–
Quadratic vs. 2FI	127.59	3	42.53	97.92	<0.0001	Suggested
Cubic vs. Quadratic	2.99	3	1.00	83.12	0.0766	Not recommended
Residual	0.048	4	0.012	–	–	–
Total	91,647.02	17	5,391.00	–	–	–
Model summary statistics						
	Std Dev.	R^2	Adj R^2	Pre R^2	PRESS	Remarks
Linear	3.20	0.8697	0.8397	0.7942	210.93	–
2FI	3.61	0.8725	0.7960	0.6230	386.35	–
Quadratic	0.66	0.9970	0.9932	0.9532	47.95	Suggested
Cubic	0.11	1.0000	0.9998	–	–	Not recommended

the main factor that would affect the deformation of a drop [36]. The drop is deformed by the excess pressure developed by the film drainage process. It is noted that the easily deformed drop has a longer film drainage time. After the breakaway/disintegration, these large oil drops travel through the pores of the medium, eventually being released at the downstream face. The large oil droplets rise to the top of the coalescing unit and enter into the decantation section. These oil droplets combine at the top of the column to form a separated layer of hydrocarbons due to the density difference and are discharged continuously via an automatic liquid level controller. The separated supernatant water is taken out continuously at a lower level (separated by 50 mm from the oil outlet) through a side outlet.

4.8. Effect of parametric interactions on oil removal efficiency of BFA bed

The individual effect of process parameters on the response (oil removal efficiency) in the design space was compared in the perturbation plot shown in Fig. 7(a). A curvature in the plot for a factor shows that the response is sensitive to that factor. It is observed that the response plots of all the three parameters, pH (*A*), bed height (*B*) and flow rate (*C*), are non-linear in nature, indicating their effect on oil removal efficiency of the BFA bed. However, the removal efficiency of oil by the BFA bed is very sensitive to pH and the bed height.

The combined effect of BFA bed height and pH on the oil removal efficiency of BFA filter media is shown by the 3D response surface plot in Fig. 8(a). It is seen that as the bed height increases, the oil removal efficiency of BFA filter media increases. At the minimum bed height of 40 mm, the oil removal efficiency of BFA filter media is the lowest because of the short residence time of the emulsion in the BFA bed. This leads to an unstable operating condition for the BFA filter media system. With an increase in BFA bed height, the column working volume increases and the oil removal efficiency of BFA filter media also increases. The maximum oil removal efficiency of 84.8% is achieved at 120 mm bed height with a flow rate of 0.135 dm^3/min and pH 2.

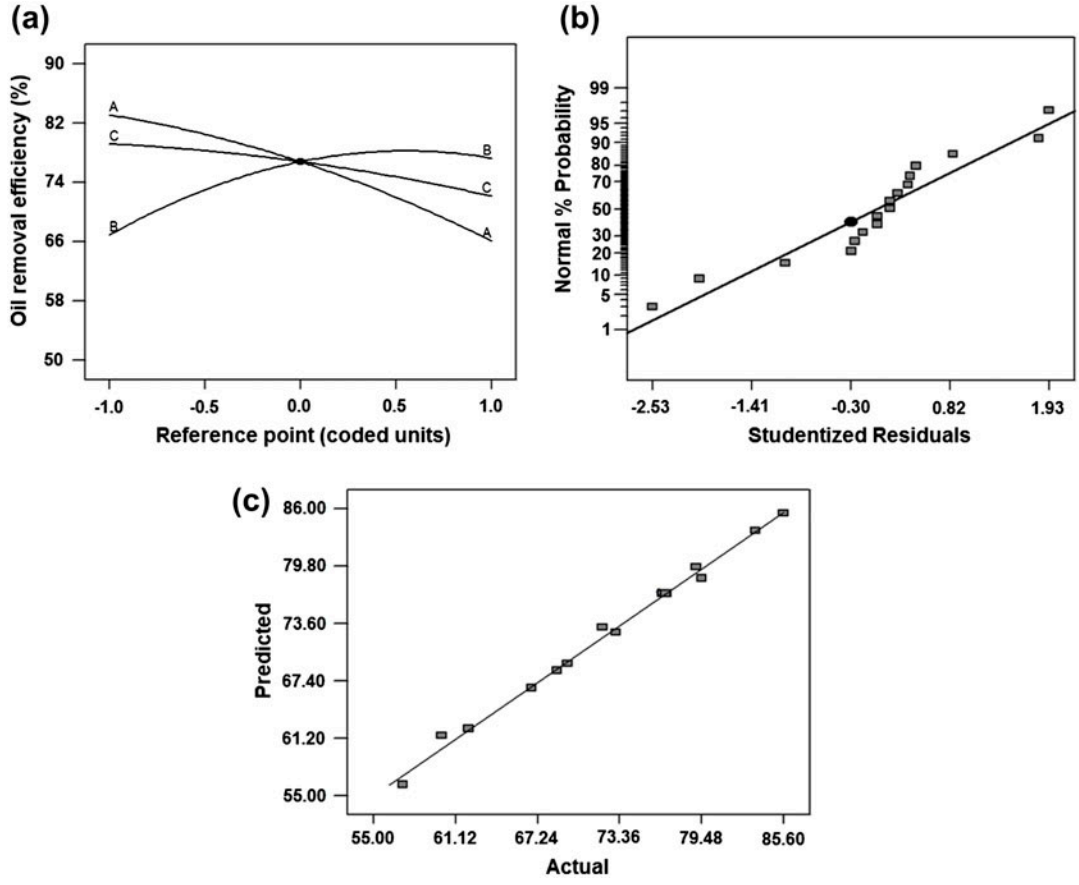

Fig. 7. (a) Perturbation plot, (b) Normal % probability vs. residual error and (c) Scatter diagram of predicted response vs. actual response for BFA filter bed system.

Table 4
Parametric constraints with model prediction and experimental values of BFA filter bed system.

Constraints	Criteria	Lower limit	Upper limit	Importance[b]	Model predicted values	Experimental values
A: pH	In range	2	10	++++	2.92	3
B: Bed height (mm)	In range	40	120	++++	101.6	100
C: Flow rate (dm^3/min) × 10^3	In range	135	270	++++	143.89	145
Y: Oil removal efficiency (%)	Maximize	–	–	++++	86.68	84.76[a]

[a]Percentage error = –2.22%.
[b]Sensitivity of response over other.

As discussed earlier (Section 4.3), when the emulsion pH < PZC (~7.8), most of the BFA particle surface becomes positively charged, due to charge interactions between the carbon graphene layers on the BFA surface and the hydronium ions [34]. The effect of initial pH_0 and the bed height on the oil removal efficiency of the filter bed is shown in Fig. 8(b).

The zeta potential of the o/w emulsion was measured as a function of pH. At pH 2, ξ of the o/w emulsion was −13.4 mV. The ξ of o/w emulsion shifts

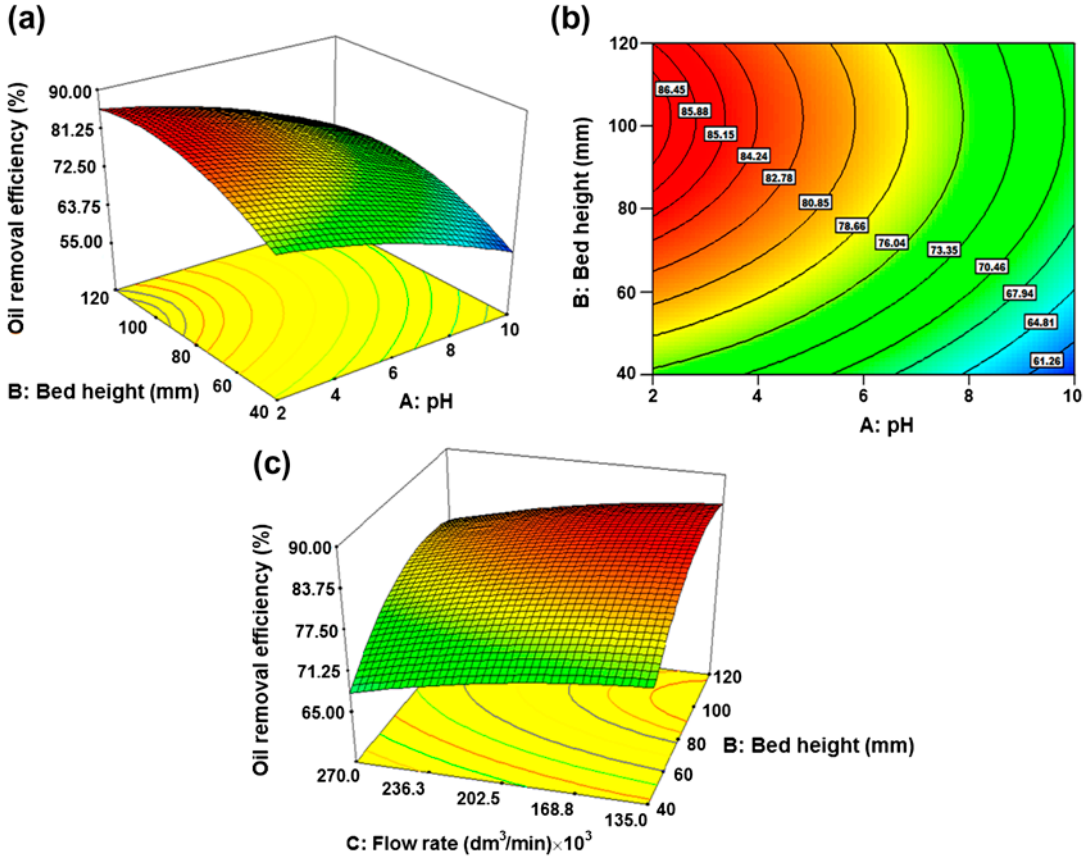

Fig. 8. (a) 3D response surface graph for oil removal efficiency vs pH and bed height for BFA filter bed system, (b) 2D contour plot for pH vs BFA bed height, and (c) 3D response surface graph for oil removal vs flow velocity and bed height of BFA filter bed system.

towards higher negative value with an increase in pH, i.e. −40.1 mV (pH 5) and −65.4 mV (pH 10). As the magnitude of ξ increases, the degree of repulsion among the negatively charged emulsion droplets also increases. This increase in repulsion resists the aggregation of the droplets. As a consequence, the stability of the emulsion increases. Therefore, the emulsion stability increases with an increase in emulsion pH, which can be observed from the measurement of the zeta potential (ξ) of the emulsion. The pH_0 of the emulsion was adjusted by the addition of 1(N) NaOH or 1(N) HCl as per requirement. At pH_0 2, ξ of o/w emulsion was −13.4 mV, which decreased to −65.4 mV at pH_0 10. When pH_0 of the emulsion is less than PZC, most of the BFA surface becomes positively charged and the negatively charged oil droplets get adsorbed on to the BFA surface. This explains that with the system pH < PZC, oil splitting may take place and the resulting oil may get adsorbed and filtered by the BFA bed.

Fig. 8(a) shows the removal of oil as a function of pH_0 of the emulsion for $2 \le pH_0 \le 10$. At pH_0 10, oil removal is 61.4%, while at a pH_0 2, the maximum oil removal is 86.4%. At neutral pH_0, the oil removal is 76.8%. With an increase in pH_0, the magnitude of ξ progressively increases as the energy barrier of repulsive force increases simultaneously and prevents the coalescence of the emulsion droplets. This makes the emulsion highly stable. The 3D response surface plot clearly indicates that the oil removal efficiency of the BFA filter bed increases with an increase in the bed height and a decrease in pH_0.

The interactive effect of flow velocity and BFA bed height on the oil removal efficiency of the BFA filter bed is shown in Fig. 8(c). As per Bernoulli's principle, a slow-moving fluid exerts more pressure and provides higher residence time between the bed particles and the emulsion/oil droplets. Thus, at a lower flow rate, the oil removal efficiency will improve. The multi-response plot confirms that the oil removal efficiency of the BFA filter bed increases with a decrease in flow velocity and an increase in bed height. It is observed that as the emulsion flow velocity increases, the oil removal efficiency of the BFA filter bed

Table 5
Cost of various adsorbent materials used for oily wastewater treatment

Adsorbent	Price (USD/kg)
Agricultural adsorbent (saw dust, barley straw, etc.)	0.1–0.15
Bagasse fly ash	0.009
Commercial activated carbon	20.0
Commercial granular activated carbon	3.3
Commercial ion exchange resin	1.1–2.4
Hydrophobic zeolite	2.95–18.2
Silica aerogel	2.5–6.0
Spheroidal cellulose (fibers)	1.07

gradually decreases. The maximum oil removal efficiency of the BFA filter media is found at a flow rate of 0.135 dm^3/min.

4.9. Cost estimation and energy economy

The two most important factors for the oily wastewater treatment process to be economically feasible are the removal efficiency and the cost of the adsorbent used. It is difficult to estimate a reliable treatment cost of such processes because of the involvement of a number of cost components, such as pumping equipment and treatment facility. Detailed information on the treatment cost of oily wastewaters is scarce in the literature as it depends strongly on the local availability of the adsorbent, pre-processing required, treatment conditions and the recycle–reuse and life cycle concerns. BFA is abundantly available in India at almost no cost from sugar cane mills and bagasse-fired furnaces/boilers. The cost is related to BFA collection, transportation to the user site, sieving, water washing and drying and the pre-processing required, if any. Table 5 presents the cost estimates of some of the adsorbents used for oily wastewater treatment. It can be seen that the BFA is the cheapest filter medium (cost < 0.01USD/kg) for oily wastewater treatment in comparison to other commercially available adsorbents. The literature scan reveals that the oil removal efficiency of BFA is comparable to other adsorbents. The spent BFA is not recommended to be regenerated and reused again, because the regeneration cost will become more than the cost of the fresh BFA. Spent BFA, saturated with oil, can, however, be sun-dried/air-dried and then can be used as a solid co-fuel in furnaces. The spent BFA has a heating value of ~24.8 MJ/kg and can, therefore, be used as a co-fuel with coal in the incinerators/boiler furnaces/combustors to recover its energy value. The residual ash can be blended with the bio-composted manure and used in the agricultural fields to enhance the mineral content and porosity of the soil.

5. Conclusions

The oil removal efficiency of the BFA filter bed was investigated experimentally. The removal efficiency of BFA filter bed was found to be more sensitive to system pH as reflected by the initial pH (pH_0) and BFA bed height as compared to the emulsion flow rate. The proposed model equation for the BFA filter bed, with a high value of $R^2 > 99.42\%$, describes the process parametric interactions in a meaningful way and the model predictions interpret the experimental data significantly well. A maximum of 84.8% oil removal efficiency of BFA filter bed was achieved at a system pH_0 3, bed height = 100 mm and emulsion flow rate = 0.145 dm^3/min. BFA is found to be an effective filter medium for the treatment of emulsified oil from oily wastewaters. This can be used as an alternative to the costly adsorbent filter materials. Spent BFA can be used as a co-fuel in the incinerator/combustors/furnaces to recover its heating value.

Acknowledgement

The authors thank Uttam Sugar Mills Ltd. for providing the BFA free of cost for the research study. The financial support provided to one of the authors (P.K.) by the Ministry of Human Resource Development (MHRD), Government of India, during the present research work is gratefully acknowledged.

References

[1] E. Iakovleva, M. Sillanpää, The use of low-cost adsorbents for wastewater purification in mining industries, Environ. Sci. Pollut. Res. 20 (2013) 78–99.
[2] P. Kundu, V. Kumar, I.M. Mishra, Modeling the steady-shear rheological behavior of dilute to highly concentrated oil-in-water (o/w) emulsions: Effect of temperature, oil volume fraction and anionic surfactant concentration, J. Pet. Sci. Eng. 129 (2015) 189–204.
[3] N.A. Mishchuk, A. Sanfeld, A. Steinchen, Interparticle interactions in concentrate water–oil emulsions, Adv. Colloid Interface Sci. 112 (2004) 129–157.

[4] P. Kundu, A. Agrawal, H. Mateen, I.M. Mishra, Stability of oil-in-water macro-emulsion with anionic surfactant: Effect of electrolytes and temperature, Chem. Eng. Sci. 102 (2013) 176–185.
[5] R.M. Bande, B. Prasad, I.M. Mishra, K.L. Wasewar, Oil field effluent water treatment for safe disposal by electroflotation, Chem. Eng. J. 137 (2008) 503–509.
[6] Ministry of Environment and Forest Notification. Environment (Protection) Amendment Rules, (2008), (Petroleum oil Refinery) G.S.R. 186(E), Mass Based Standards for SRU in Petroleum Oil Refinery, India.
[7] J.M. Benito, G. Rios, C. Pazos, J. Coca, Methods for the separation of emulsified oil from water: A state-of-the-art review, Trends Chem. Eng. 4 (1998) 203–231.
[8] V.K. Sangal, I.M. Mishra, J.P. Kushwaha, Electrocoagulation of soluble oil wastewater: Parametric and kinetic study, Sep. Sci. Technol. 48 (2013) 1062–1072.
[9] S. Maiti, I.M. Mishra, S.D. Bhattacharya, J.K. Joshi, Removal of oil from oil-in-water emulsion using a packed bed of commercial resin, Colloids Surf., A: Physicochem. Eng. Aspects 389 (2011) 291–298.
[10] P. Kundu, I.M. Mishra, Removal of emulsified oil from oily wastewater (oil-in-water emulsion) using packed bed of polymeric resin beads, Sep. Purif. Technol. 118 (2013) 519–529.
[11] T. Viraraghavan, G.N. Mathavan, Treatment of oily waters using peat, Water Pollut. Res. J. Canada 25 (1990) 73–90.
[12] G.N. Mathavan, T. Viraraghavan, Coalescence/filtration of an oil-in-water emulsion in a peat bed, Water Res. 26 (1992) 91–98.
[13] C. Solisio, A. Lodi, A. Converti, M. Del Borghi, Removal of exhausted oils by adsorption on mixed Ca and Mg oxides, Water Res. 36 (2002) 899–904.
[14] A. Cambiella, E. Ortea, G. Rios, J.M. Benito, C. Pazos, J. Coca, Treatment of oil-in-water emulsions: Performance of a sawdust bed filter, J. Hazard. Mater. 131 (2006) 195–199.
[15] M. Achak, L. Mandi, N. Ouazzani, Removal of organic pollutants and nutrients from olive mill wastewater by a sand filter, J. Environ. Manage. 90 (2009) 2771–2779.
[16] M. Sadeghian, M. Sadeghi, M. Hesampour, A. Moheb, Application of response surface methodology (RSM) to optimize operating conditions during ultrafiltration of oil-in-water emulsion, Desalin. Water Treat. 55 (2015) 615–623.
[17] J. Mueller, Y. Cen, R.H. Davis, Crossflow microfiltration of oily water, J. Membr. Sci. 129 (1997) 221–235.
[18] M. Abbasi, A. Salahi, M. Mirfendereski, T. Mohammadi, F. Rekabdar, M. Hemmati, Oily wastewater treatment using mullite ceramic membrane, Desalin. Water Treat. 37 (2012) 21–30.
[19] H. Rogues, Y. Aurello, Oil-water Separations: Oil Recovery and Oily Wastewater Treatment, Kluwer Academic Publisher, Netherlands, 1991.
[20] L.A. Spielman, Y.P. Su, Coalescence of oil-in-water suspensions by flow through porous media, Ind. Eng. Chem. Fundam. 16 (1977) 272–282.
[21] J. Li, Y.A. Gu, Coalescence of oil-in-water emulsions in fibrous and granular beds, Sep. Purif. Technol. 42 (2005) 1–13.
[22] M.M. Swamy, I.D. Mall, B. Prasad, I.M. Mishra, Sorption characteristics of O-cresol on bagasse fly ash and activated carbon, Int. J. Environ. Health 40 (1998) 67–78.
[23] V.C. Srivastava, M.M. Swamy, I.D. Mall, B. Prasad, I.M. Mishra, Adsorptive removal of phenol by bagasse fly ash and activated carbon: Equilibrium, kinetics and thermodynamics, Colloids Surf., A: Physicochem. Eng. Aspects 272 (2006) 89–104.
[24] D.H. Lataye, I.M. Mishra, I.D. Mall, Removal of pyridine from aqueous solution by adsorption on bagasse fly ash, Ind. Eng. Chem. Res. 45 (2006) 3934–3943.
[25] D.H. Lataye, I.M. Mishra, I.D. Mall, Adsorption of 2-picoline onto bagasse fly ash from aqueous solution, Chem. Eng. J. 138 (2008) 35–46.
[26] A. Kumar, B. Prasad, I.M. Mishra, Optimization of acrylonitrile removal by activated carbon-granular using response surface methodology, Can. J. Chem. Eng. 87 (2009) 637–643.
[27] A. Kumar, B. Prasad, I.M. Mishra, Process parametric study for ethane carboxylic acid removal onto powder activated carbon using Box-Behnken Design, Chem. Eng. Technol. 30 (2007) 932–937.
[28] Z.Y. Ooi, N. Othman, N.F. Mohamed, Noah, Response surface optimization of kraft lignin recovery from pulping wastewater through emulsion liquid membrane process, Desalin. Water Treat. (in press), doi:10.1080/19443994.2015.1024754.
[29] M. Rajasimman, P. Karthic, Application of response surface methodology for the extraction of chromium (VI) by emulsion liquid membrane, J. Taiwan Inst. Chem. Eng. 41 (2010) 105–110.
[30] IS 1350, (Part I) Methods of Test for Coal and Coke Proximate Analysis, Bureau of Indian Standards, Manak Bhawan, New Delhi, India, 1984.
[31] IS 355, Methods of Determination of Chemical Composition of Ash of Coal and Coke, Bureau of Indian Standards, Manak Bhawan, New Delhi, India, 1974.
[32] I.D. Mall, V.C. Srivastava, N.K. Agarwal, I.M. Mishra, Adsorptive removal of malachite green dye from aqueous solution by bagasse fly ash and activated carbon-kinetic study and equilibrium isotherm analyses, Colloids Surf., A: Physicochem. Eng. Aspects 264 (2005) 17–28.
[33] B.R. Puri, P.L. Walker (Eds.), Chemistry and Physics of Carbon, Marcel Dekker, New York, NY, 1966.
[34] C. Leon y Leon, J.M. Solar, V. Calemma, L.R. Radovic, Evidence for the protonation of basal-plane sites on carbon, Carbon 30 (1992) 797–811.
[35] R.H. Myers, C.M. Montgomery, Response Surfaces Methodology: Process and Product Optimization using Designed Experiments, Wiley, New York, NY, 1995.
[36] H.M. Princen, Shape of a fluid drop at a liquid-liquid interface, J. Colloid Sci. 18 (1963) 178–195.